



## Original Research Article

# Thermal decomposition of ammonium perchlorate-commercial nano-TiO<sub>2</sub> mixed powder

Mostafa Mahinroosta 

School of Chemical, Petroleum, and Gas Engineering, Iran University of Science and Technology

### ARTICLE INFORMATION

Receive: 11 September 2018  
 Received in revised: 15 October 2018  
 Accepted: 2 November 2018  
 Available online: 7 February 2019

DOI: [10.26655/AJNANOMAT.2019.2.3.3](https://doi.org/10.26655/AJNANOMAT.2019.2.3.3)

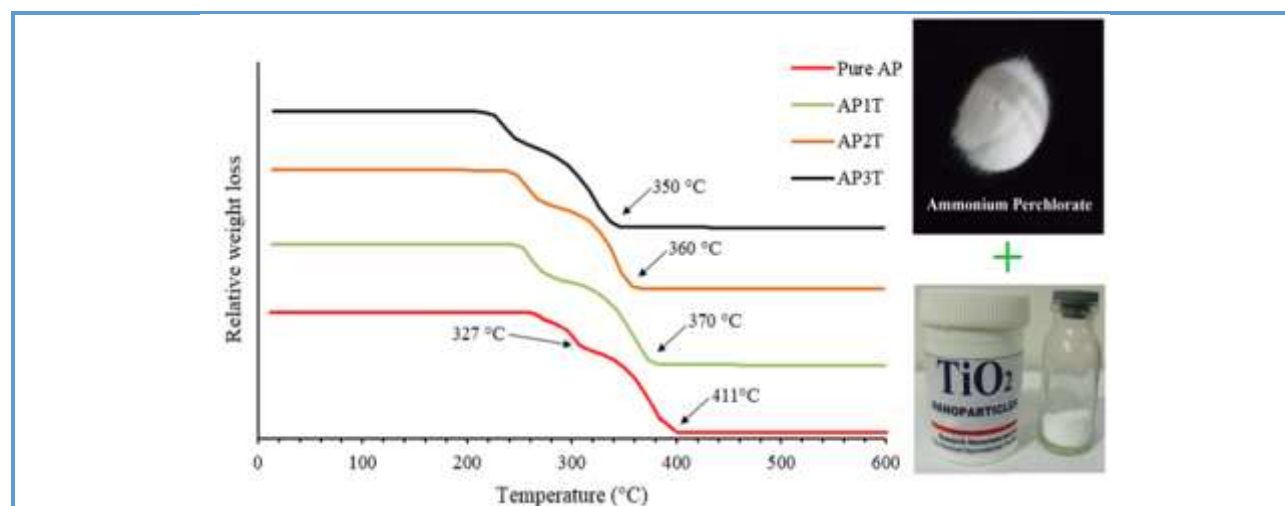
### KEYWORDS

Titania  
 Ammonium perchlorate  
 Thermal decomposition  
 Nanoparticle

### ABSTRACT

Thermal decomposition of ammonium perchlorate was improved via addition of transition metals and metal oxides. This work investigates the thermal decomposition of the ammonium perchlorate under the catalytic effect of the commercial nano-TiO<sub>2</sub> (nTiO<sub>2</sub>). Characterization of nTiO<sub>2</sub> showed that its average particle size ranged from 10 to 25 nm with a relatively spherical morphology. Ammonium perchlorate and nTiO<sub>2</sub> mixes were prepared by adding three different nTiO<sub>2</sub> mass fractions of 1, 2, and 3 wt% to pure ammonium perchlorate. The results of thermogravimetry analysis revealed that the addition of nTiO<sub>2</sub> to pure ammonium perchlorate resulted in a significant decline in its decomposition temperature. The most observed decrease in the decomposition temperature was 61 °C resulted from the addition of 3 wt.% nTiO<sub>2</sub>.

## Graphical Abstract



## Introduction

Over the last few years, nanoparticles of many different compounds and combinations have received considerable attention in the scientific and engineering research fields [1]. Nanometer materials exhibit a much larger surface area for a certain mass or volume compared to conventional particles [2]. The oxide nanoparticles are the materials with good electrical, optical, magnetic, and catalytic properties that are different from their bulk counterparts [3]. Reduction in the particle size lessens the transient heat conduction travel through the particle over time, and an increase in the surface-to-volume ratio leads to better dispersion of the particles in the mixture, increasing the reactant sites. Finally, the nanometer particles can have a completely different surface chemistry, often better than their micron-sized counterparts [4]. Among these nanostructure oxides, titanium dioxide or titania ( $\text{TiO}_2$ ) nanostructures have emerged as one of the most promising materials because of their potential for gas sensors, especially for humidity and oxygen detection [2, 3, 5], optical devices [3, 5, 6], photocatalysis [2, 3, 6], fabricating capacitors in microelectronic devices due to its unusually high dielectric constant [3, 6], pigments [2, 7], adsorbents [7], and solar cells [5]. A relatively low level of  $\text{TiO}_2$  is needed to achieve a white opaque coating which is resistant to discoloration under ultraviolet light.  $\text{TiO}_2$  pigment is used in many diverse products, such as paints, coatings, glazes, enamels, plastics, papers, inks, fibers, foods, pharmaceuticals or cosmetics. Pure

titanium dioxide is colorless in the massive state, non-toxic, thermally stable, inert versus acids, alkalis and solvents. It exists under three fundamental crystalline phases: rutile which is the most stable and the most abundant form, anatase (octahedrite) and brookite. All three forms occur naturally but the latter is rather rare and has no commercial interest. Anatase becomes more stable than rutile when the particle size is decreased below 14 nm. Generally speaking, the functional properties of nano- $\text{TiO}_2$  are influenced by a large number of factors such as particle size, surface area, synthesis method and conditions, and crystallinity [2].

$\text{TiO}_2$  may have a positive catalytic effect on the improvement of some important chemical reactions such as thermal decomposition of ammonium perchlorate (AP). This idea can be brightened by a glimpse into the catalytic effects of transition metals and metal oxides on the above-mentioned reaction. Since the AP is used for the preparation of energetic materials, investigating its thermal decomposition behavior is of a great importance. Any improvement in the thermal decomposition of AP may lead to an improvement in burning rate of energetic materials. Thus, many researchers have focused on this field of research and concluded that the presence of nano metals and/or metal oxides, especially transition metal oxides, as the nanocatalyst tailors the thermal decomposition of AP [8–10]. The decrease in decomposition temperature of AP in the presence of the different nano metal and metal oxides are presented in Table 1.

**Table 1.** Some reported data from the literature on the decline in AP decomposition temperature in the presence of various nano metal or metal oxides

Nanocatalyst	Preparation method	wt.%	Decrease in decomposition temperature (°C)	Ref.
Nano-yttria	Sol-gel	5	114.6	[11]

CuO/AP composite nanoparticles	A novel solvent-nonsolvent method	-	95.83	[12]
Co <sub>2</sub> O <sub>3</sub> /AP composite nanoparticles	A novel solvent-nonsolvent method	-	137.11	[12]
NiO nanoparticles	Solid-state reaction	2	93	[13]
Ni nanoparticles	Hydrogen plasma method	2-5	92-105	[14]
Nano-sized MgO	Sol-gel	2	75	[15]
Nano-sized $\alpha$ -Fe <sub>2</sub> O <sub>3</sub>	Electrochemical method	2	59	[16]
Nanometer CoFe <sub>2</sub> O <sub>4</sub>	Polyol-medium solvothermal	2	112.8	[17]
Nano-MnFe <sub>2</sub> O <sub>4</sub>	Co-precipitation phase inversion	3	77.3	[18]
Nano-MnFe <sub>2</sub> O <sub>4</sub>	Low-temperature combustion	3	84.9	[18]
Sphere-like $\alpha$ -Fe <sub>2</sub> O <sub>3</sub>	NH <sub>3</sub> ·H <sub>2</sub> O and NaOH solution to adjust the pH value	-	81	[19]
pod-like $\alpha$ -Fe <sub>2</sub> O <sub>3</sub>	NH <sub>3</sub> ·H <sub>2</sub> O and NaOH solution to adjust the pH value	-	72	[19]
Nanometer CoC <sub>2</sub> O <sub>4</sub>	Co-precipitation	2	104	[20]
Nano-sized CuO	Sol-gel	-	90.47	[21]
Nano-sized Co <sub>3</sub> O <sub>4</sub>	Sol-gel	-	92.07	[21]
Nano-sized CuCo <sub>2</sub> O <sub>4</sub>	Sol-gel	-	102.78	[21]
CuO nanocrystals	Simple chemical deposition	2	85	[22]
Nanometer CuFe <sub>2</sub> O <sub>4</sub>	Auto-combustion method	2	105	[23]
Co nanoparticles	Hydrogen plasma	2	145.01	[24]
Cu-Co nanocrystal	Hydrazine reduction	1	96	
Cu-Fe	in ethylene glycol	1	89	
Cu-Zn		1	114	[25]

Also, some recent studies have been conducted on the catalytic effect of nano-MnO<sub>2</sub> [26], nano-M<sub>x</sub>O<sub>y</sub> (M=Mn, Fe) [27], Co<sub>3</sub>O<sub>4</sub> nanowires [28], CuO/Al<sub>2</sub>O<sub>3</sub> composite [29], flower-like ZnO@Fe<sub>2</sub>O<sub>3</sub> nanostructures [30], and hierarchical flower-like Co<sub>3</sub>O<sub>4</sub> [31] on the thermal decomposition of AP. All these studies reported more than 100 °C decrease in the pyrolysis temperature of AP. Vargeese [32] indicated that TiO<sub>2</sub> has a strong catalytic effect on the thermal decomposition of AP. Fujimura

and Miyake [33] investigated the influence of specific surface area of TiO<sub>2</sub> on the thermal decomposition of AP. They expressed that as the specific surface area of TiO<sub>2</sub> increases, thermal decomposition temperature of AP diminishes. Within the scope of this study, the catalytic effect of commercial nTiO<sub>2</sub> on the thermal decomposition of AP is probed.

## Experimental

### Materials and methods

Ammonium perchlorate (AP) was purchased from Merck. It was monomodal with the particle size of 120  $\mu\text{m}$ . Commercial  $\text{nTiO}_2$  was purchased from Pishgaman Company, Mashhad,

Iran. It was in anatase form and its purity was more than 99%. Tables 2 and 3 show the chemical analysis of the impurities and physical properties of  $\text{nTiO}_2$ , respectively.

**Table 2.** Chemical impurities of  $\text{nTiO}_2$

Element	Mg	Nb	Al	S	Si	Ca
Amount (ppm)	$\leq 67$	$\leq 82$	$\leq 19$	$\leq 128$	$\leq 116$	$\leq 75$

**Table 3.** Physical properties of  $\text{nTiO}_2$

Bulk density ( $\text{g}/\text{cm}^3$ )	Actual density ( $\text{g}/\text{cm}^3$ )	Average particle size (nm)	Specific surface area ( $\text{m}^2/\text{g}$ )
0.24	3.90	10-25	200-240

### Sample preparation

The AP/ $\text{nTiO}_2$  mixtures were prepared with various mass loadings of  $\text{nTiO}_2$  namely 1, 2, and 3 wt.% for the evaluation of the thermal decomposition of AP. The mixtures were labeled as AP1T (AP+1%  $\text{nTiO}_2$ ), AP2T (AP+2%  $\text{nTiO}_2$ ), and AP3T (AP+3%  $\text{nTiO}_2$ ). The samples were manually homogenized before any thermal decomposition experiments.

### Characterization techniques

X-ray diffractogram of the  $\text{nTiO}_2$  was recorded using a powder X-ray diffractometer (Philips PW 1800) with Cu-K $\alpha$  radiation at 40 kV and 30 mA. The morphology of  $\text{nTiO}_2$  particles was disclosed using SIGMA VP-500 FESEM microscope (ZEISS) at 15 kV. A thermogravimetry analyzer (Dupont 2000) was employed to study the thermal decomposition of the as-prepared mixtures at a heating rate of 10  $^\circ\text{C}/\text{min}$  from room temperature until 600  $^\circ\text{C}$ .

## Results and Discussion

### Characterization of $\text{nTiO}_2$

Figure 1 depicts the X-ray diffractogram of the commercial  $\text{nTiO}_2$ . It can clearly be seen that diffraction peaks in the pattern are associated

with the anatase phase with an appropriate crystalline nature. A very intense anatase peak is observed at  $2\theta$  of  $25.25^\circ$ , assigned to (101) plane. Other anatase peaks appeared at  $2\theta$  of  $37.7^\circ$  (004),  $47.7^\circ$  (200),  $53.54^\circ$  (105), and  $62.32^\circ$  (204).

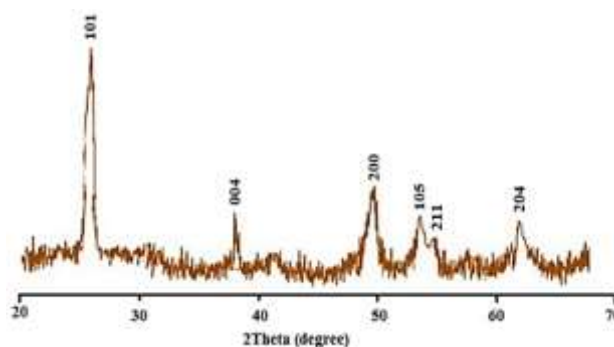


**Figure 1.** XRD pattern of  $\text{nTiO}_2$

The field emission scanning electron microscopy (FESEM) micrographs were obtained to reveal the morphology of the particles. The obtained FESEM images are displayed in Figure 2. It is obvious from the micrographs that the  $\text{nTiO}_2$  particles are agglomerations of relatively spherical particles.

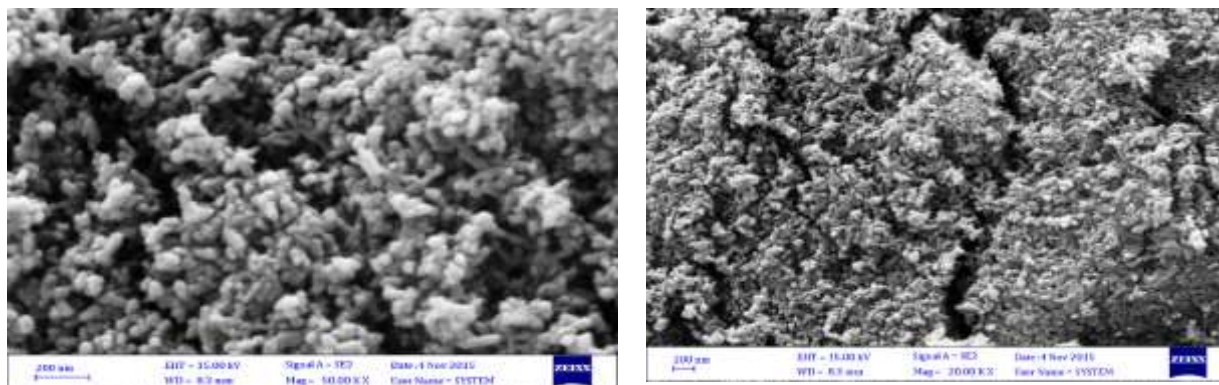


**Figure 2.** FESEM images of nTiO<sub>2</sub>

### *Effect of nTiO<sub>2</sub>*

Figure 3 indicates the TGA results of the pure AP and AP/nTiO<sub>2</sub> mixtures. As can be observed in the curve related to pure AP, the first exothermic peak appeared at 327 °C that accompanied by a weight loss of around 18%. This peak is associated with the partial

decomposition of AP and the formation of some amounts of NH<sub>3</sub> and HClO<sub>4</sub> via dissociation and sublimation. The second exothermic peak took place at 411 °C, corresponding to a weight loss of about 92%. In this stage, transition products are completely decomposed to volatile products.

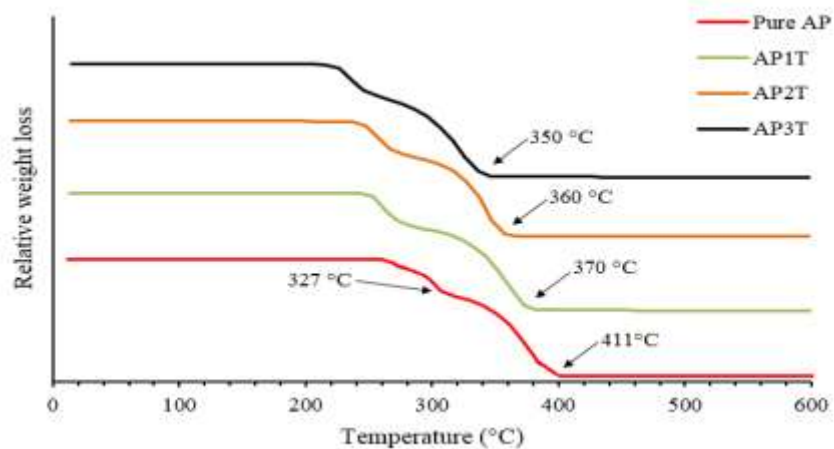


**Figure 3.** TGA curves of pure AP and AP/nTiO<sub>2</sub> mixtures

According to the TGA curves of AP/nTiO<sub>2</sub> mixtures, it is clear that the partial decomposition of AP in the presence of 1, 2, and 3 wt.% of nTiO<sub>2</sub> happened at a temperature much lower than 327 °C. Also, complete decomposition of AP in the presence of 1, 2, and 3 wt.% of nTiO<sub>2</sub> occurred at temperatures of 370, 360, and 350 °C, respectively. These temperatures are accompanied by a decline of

41, 51, and 61 °C, respectively. It is obvious that addition of nTiO<sub>2</sub> to pure AP has a deep effect on its exothermic decomposition. According to these results, it can be concluded that the catalytic effect of nTiO<sub>2</sub> is observed mainly on high-temperature decomposition stage and not on the initial stages of decomposition.

Despite the very good catalytic activity of the nanomaterials listed in Table 1 and also some

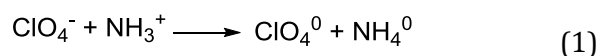


recent results, the nTiO<sub>2</sub> has advantages such as lower price, availability and ease of synthesis, making this inorganic oxide more attractive for real applications.

#### Mechanism of thermal decomposition of AP

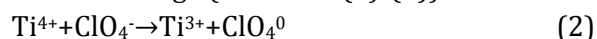
Two main mechanisms have been suggested for thermal decomposition of the AP [11, 16, 17, 21]:

The first mechanism is based on hypothesis of electron transfer from perchlorate ion to ammonium ion which is as follows:



The high electron transfer capacity and the large specific surface area of nTiO<sub>2</sub> play a significant role in the acceleration of the thermal decomposition of AP. The occurrence of reaction (1) can be explained as follows: Titanium has the electronic configuration of [Ar]3d<sup>2</sup>4s<sup>2</sup>. Experiments have demonstrated that Ti can form +2, +3 and +4 oxidation states, so it can lose 2, 3 or 4 electrons

to form cations. The +4 state is the most common and stable, because it is able to form an octet. The +3 state is less stable (more reactive) because it leaves a single d electron in the valence orbital. Ti<sup>4+</sup> cation in TiO<sub>2</sub> structure has s- and d-type orbitals with 3d<sup>0</sup>4s<sup>0</sup> electronic configuration. These orbitals have not been filled with electrons and therefore provide an appropriate space for electron transfer in AP thermal decomposition process and play the role of a bridge (reactions (2)-(5)).



By accepting electrons transferred from ClO<sub>4</sub> degradation, ClO<sub>4</sub> degradation is promoted. On the other hand, commercial nTiO<sub>2</sub> has a large specific surface area and large amount of active sites. These sites increase adsorption of the reactive molecules in gas phase to the surface and promote the redox reactions between them. Figure 4 illustrates a schema of the above-mentioned mechanism.

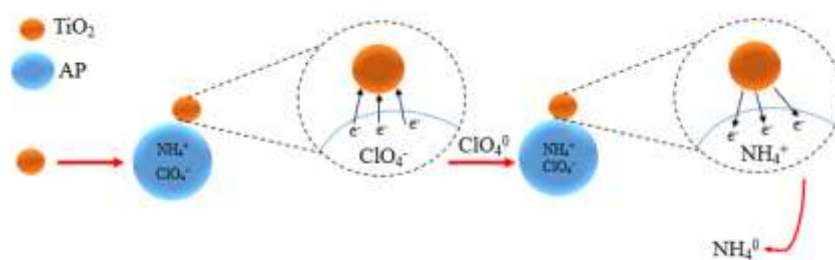
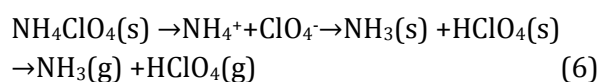


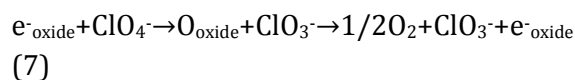
**Figure 4.** A schema of electron transfer mechanism by TiO<sub>2</sub>

The second mechanism relies on proton transfer from ammonium ion to perchlorate ion which is as follows:



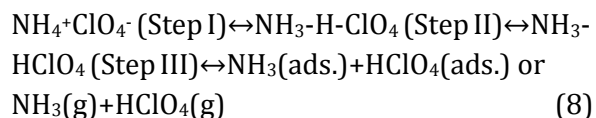
For the first mechanism, it is proposed that the rate-determining step is electron transfer and

inasmuch as the p-type semiconductors have positive holes, they can accept the released electron from perchlorate ion. Thus, these catalysts accelerate the electron transfer.



where  $e^-_{\text{oxide}}$  is a positive hole in the valence band of the oxide and  $O_{\text{oxide}}$  is an abstracted oxygen atom from oxide. It is clear that this mechanism includes two steps: 1) oxidation of ammonia and 2) dissociation of  $\text{ClO}_4^-$  species into  $\text{ClO}_3^-$  and  $\text{O}_2$ .

In first step, metal oxides exhibited high catalytic activity in ammonia oxidation and in second step metal oxides accepted the released electron from ammonia oxidation that may promote the dissociation of  $\text{ClO}_4^-$  into  $\text{ClO}_3^-$  and  $\text{O}_2$ . For the second mechanism, steps (I)-(III) were proposed. In step (I), the ammonium and perchlorate ions were paired. Step (II) starts with proton transfer from  $\text{NH}_4^+$  cation to  $\text{ClO}_4^-$  anion and thus a molecular complex was formed. The formed complex was finally decomposed into  $\text{NH}_3$  and  $\text{HClO}_4$  in step (III). The molecules of  $\text{NH}_3$  and  $\text{HClO}_4$  either reacted on the perchlorate surface or they are desorbed and sublimed that is accompanied by interactions in gas phase.



At low temperature (<350 °C), the surface reaction was performed more rapidly compared with the sublimation in gas phase.

Based on the proton transfer, during high-temperature decomposition, the nanoparticles adsorb the reactive molecules on their surface and catalyze the reaction. The existence of more holes in p-type semiconductor catalysts is responsible for the increasing of the AP decomposition.

## Conclusions

Thermal decomposition of the ammonium perchlorate was investigated in the presence of the nano-TiO<sub>2</sub>. For this purpose, three different ammonium perchlorate/nano-TiO<sub>2</sub> mixtures were prepared by adding various mass

fractions of nano-TiO<sub>2</sub> to pure ammonium perchlorate. The thermal decomposition experiments were then performed using thermogravimetry analysis. The results indicated that the nano-TiO<sub>2</sub> had a significant catalytic effect on the thermal decomposition of ammonium perchlorate. By increasing the nano-TiO<sub>2</sub> mass fraction, a greater decline in decomposition temperature of ammonium perchlorate, especially at the second exothermic stage was achieved. An electron transfer mechanism was proposed, as well.

## Orcid

Mostafa Mahinroosta  0000-0001-9709-294

## References

- [1]. Nikam A.P., Ratnaparkhiand M.P., Chaudhari S.P. *Int. J. Res. Dev. Pharm Life Sci.*, 2014, **3**:1121
- [2]. Marie-Isabelle B. *Open Nanosci J.*, 2013, **5**:64
- [3]. Suresh S. *Am. J. Nanosci Nanotechnol*, 2013, **1**:27
- [4]. Biener J., Wittstock A., Baumann T.F., Weissmüller J., Bäumer M., Hamza A.V. *Mater*, 2009, **2**:2404
- [5]. MortezaAli A., Saeideh R.S. *J. Nanostruct Chem.*, 2013, **3**:35
- [6]. Karimi L., Zohoori S. *J. Nanostruct Chem.*, 2013, **3**:32
- [7]. Vijayalakshmi R., Rajendran V. *Archives Appl. Sci. Res.*, 2012, **4**:1183
- [8]. Chen Y., Ma K., Wang J., Gao Y., Zhu X., Zhang W. *Mater Res. Bull.*, 2018, **101**:56
- [9]. Ramdani Y., Liu Q., Huiquan G., Liu P., Zegaoui A., Wang J. *Vacuum*, 2018, **153**:277
- [10]. Chen L., Zhu D. *Ceram Int.*, 2015, **41**:7054
- [11]. Chen W., Li F., Liu L., Li Y. *J. Rare Earths*, 2006, **24**:543
- [12]. Zhenye M.A., Fengsheng L., Aisi C. *Nanosci*, 2006, **11**:142
- [13]. Yanping W., Junwu Z., Xujie Y., Lude L., Xin W. *Thermochimica Acta.*, 2005, **437**:106

- [14]. Hungzhen D., Xiangyang L., Guanpeng L., Lei X., Fengsheng L. *Mater Process Technol*, 2008, **208**:494
- [15]. Guorong D., Xujie Y., Jian C., Guohong H., Lude L., Xin W. *Powder Technol*, 2007, **172**:27
- [16]. Satyawati S.J., Prajakta R.P., Krishnamurthy V.N. *Def. Sci. J.* 2008, **58**:721
- [17]. Zhao S., Ma D. *J. Nanomat.*, 2010, 2010:5 pages
- [18]. Han A., Liao J., Ye M., Li Y., Peng X. *Chin. J. Chem. Eng.*, 2011, **19**:1047
- [19]. Yifu Z., Xinghai L., Jiaorong N., Lei Y., Yalan Z., Chi H. *J. Solid State Chem.*, 2011, **184**:387
- [20]. Yu Z., Chen L., Lu L., Yang X., Wang X. *Chin. J. Catal.*, 2009, **30**:19
- [21]. Alizadeh-Gheshlaghi E., Shaabani B., Khodayari A., Azizian-Kalandaragh Y., Rahimi R. *Powder Technol*, 2012, **217**:330
- [22]. Wang J., He S., Li Z., Jing X., Zhang M., Jiang Z. *J. Chem. Sci.*, 2009, **121**:1077
- [23]. Liu T., Wang L., Yang P., Hu B. *Mater Lett.*, 2008, **62**:4056
- [24]. Duan H., Lin X., Liu G., Xu L. *Chin. J. Chem. Eng.*, 2008, **16**:325
- [25]. Pratibha S., Reena D., Kapoor I.P.S., Singh G. *Indian J. Chem.*, 2010, **49A**:1339
- [26]. Chen Y., Ma K., Wang J., Gao Y., Zhu X., Zhang W. *Mater Res. Bull.*, 2018, **101**:56
- [27]. Mahdavi M., Farrokhpour H., Tahriri M. *Mater Chem. Phys.*, 2017, **196**:9
- [28]. Yu C., Zhang W., Gao Y., Chen Y., Ma K., Ye J., Shen R., Yang Y. *Mater Res. Bull.*, 2018, **97**: 483
- [29]. Paulose S., Raghavan R., George B.K. *J. Ind. Eng. Chem.*, 2017, **53**:155
- [30]. Bu X., Liu F., Zhang Z., Wang Z., Liu J., Liu W. *Mater Lett.*, 2018, **219**:33
- [31]. Li G., Bai W. *Chem. Phys.*, 2018, **506**:45
- [32]. Vargeese A. *Mater Chem. Phys.* 2013, **139**:537
- [33]. Fujimura K., Miyake A. *J. Therm Anal. Calorim*, 2010, **99**:27

ammonium perchlorate-commercial nano-TiO<sub>2</sub> mixed powder. *Asian Journal of Nanoscience and Materials*, 2019, 2(3), 278-285. DOI: [10.26655/AJNANOMAT.2019.2.3.3](https://doi.org/10.26655/AJNANOMAT.2019.2.3.3)

**How to cite this manuscript:** Mostafa Mahinroosta\*. Thermal decomposition of